RSC Advances

ROYAL SOCIETY OF CHEMISTRY

www.rsc.org/advances

ARTICLE TYPE www. rsc.org/xxxxxx | XXXXXXXX

Quick low temperature coalescence of Pt nanocrystals on silica exposed to NO - the case of reconstruction driven growth ?

Zbigniew Kaszkur,*[a] Bogusław Mierzwa,[a] Wojciech Juszczyk,[a] Piotr Rzeszotarski,[a] and Dariusz Łomot[a]

Received Xth XXXXXXXXXX 20XX, Accepted Xth XXXXXXXXX 20XX
First published on the web Xth XXXXXXXXXX 200X
DOI: 10.1039/b000000x

We report operando XRD/MS experiment on nanocrystalline Pt supported on silica monitoring quick growth of Pt in NO atmosphere. XRD data following NO flow show structural changes typical for surface reconstruction. This would mean that although small pressure of NO lifts surface reconstruction of clean surface, the higher pressure of NO causes surface to reconstruct again. TEM photographs show formation of clusters of Pt nanoparticles pointing to growth controlled by coalescence. As surface reconstruction is the phenomenon we always see accompanying quick growth we postulate mechanism of self-lifting cyclic reconstruction that drives transport of whole clusters and their fusion.

1 Introduction

Due to use of Pt in automotive catalysts for abatement of NO_x from engine vehicle exhaust, the interaction of NO with Pt surface is of great technological importance. Also high loses of Pt during commercial plant nitric acid production are still a high cost problem and the reaction runs in substantial NO concentration. In all these processes Pt surface reconstruction phenomena play significant but not fully understood role. In explaining atomistic mechanisms of these processes a crucial contribution had surface science vacuum techniques. It is however growing awareness that to fully understand practical reactions, normal to high pressure experimental techniques are needed and that the high pressure condition makes a difference for the atomistic picture of the adsorbate layer[1]. A range of helpful techniques have been developed in recent years (e.g. Frequency Sum Generation[2,3], High Pressure STM[4,5]) but as versatile and direct technique as powder diffraction seems to be undervalued and neglected in surface studies. However XRD, when applied in situ to nanocrystalline material can provide sensitive data that to large extent relate to crystalline surface and can be well understood and interpreted with little help of atomistic simulations[6,7]. Using this technique e.g. we have shown time evolution of surface reconstruction of Pt during desorption of H_2 and the magnitude of the measured response could be scaled to the particle size[8].

We present here an operando XRD/MS study of sintering of Pt nanocrystals supported on silica in NO atmosphere and at moderate temperatures. Surprisingly we observe quick, stepwise growth of Pt nanocrystals at temperature 353 K and above, controlled at a given temperature by the time of exposition to NO. During this process transmission electron microscopy shows clearly separate Pt crystallites forming clusters on the way to grow to larger size.

A rapid sintering in NO has been already observed for Pt supported on $\gamma - Al_2O_3$ at 473 K[9] what may suggest that for the effect, if support related, the difference between the oxide supports is irrelevant. For Pt/Al_2O_3[9] the authors suggest Pt atoms transport mechanism through emission (vaporization) from small Pt clusters- the mechanism resembling Ostwald ripening. The suggested migrating species are volatile NO containing Pt complexes. This may add to understanding the experimental observation of weight loss of a platinum gauze during ammonia oxidation approaching constant value at temperatures falling down from 1170 K to 1000 K[10]. During ammonia oxidation, NO is an intermediate product interacting with O_2 and the catalyst. The loss occurs in oxidizing environment and may resemble a weight loss of Pt foil heated in air[11] attributed to volatile PtO_2. Oxygen however, at 473 K affects Pt crystal growth with much less rate of the process than NO[9]. It is expected that the Pt emission at a given temperature should be more likely for Pt nanoclusters than for larger crystals. The literature offers not much data on possible complexes of Pt containing NO although some unstable nitrosyl complexes are likely to exist. Our experiments show rapid sintering at as small temperatures as 353 K (80 deg.C) and the rate rather weakly depends on temperature up to 473 K. Above this temperature no further sintering was observed. A rapid sintering of metal nanocrystals supported on silica in NO atmosphere we observe for Pt but never for Pd metal. It also has not been observed in CO

[a] *Institute of Physical Chemistry PAS,Kasprzaka 44/52, 01-224, Warszawa, Poland. Fax: 48 223433450; Tel: 48 223433284; E-mail: zbig@ichf.edu.pl*

atmosphere. During Pt/SiO_2 exposure to NO at 80 deg.C dissociation of NO leads to a noticeable evolution of N_2O and O_2.

Our results suggest sintering mechanism of Pt on silica slowly changing with temperature, at lowest temperatures (353 K) being of a whole cluster transport followed by clusters coalescence that is a rate determining process. This observation contradicts a general opinion that sintering can be a rate determining process only at high temperature with lower temperature growth controlled by diffusion[12]. Since a moderate increase of temperature triggers still further particle growth, the pore structure of the support is here not an important limiting factor and crystallites are allowed to migrate to grow by coalescence on collision. This unexpected mobility and sintering may be ascribed to a specific character of NO chemisorption.

NO has a similar electronic structure to CO but with extra unpaired electron in its $2\pi^*$ orbital. An interaction with transition metal surface is via hybridization of molecular 5σ levels with unoccupied d states (sigma donation) and hybridization of a molecular $2\pi^*$ levels with occupied d states (pi backbonding). The latter effect dominates for Pd and Pt.

NO may dissociate at the Pt crystallite surface even at room temperature[13] but this ability strongly depends on the crystal face exposed. The dissociated species may associate into desorbing N_2O with low activation barrier and much less likely to gaseous N_2[14]. Although there is no evidence of non-dissociative sorption of NO on silica, small amounts of O_2 released together with N_2O from the metal, may cause formation of NO_2 layer strongly sorbed on the support[15] weakening adhesion forces between Pt clusters and the support and reducing the activation energy for surface migration. On the other hand the chemisorption of NO on Pd at RT is mostly associative and only a small fraction of molecules may dissociate on defects of the metal structure[16].

Pd as well as other 4d metals differs from 5d metals in the latter having the ability of crystal surface to easily reconstruct[17,18]. It is e.g. known that clean (110) face of Pt undergoes so called missing-raw reconstruction[19] whereas chemisorption of gases lifts this reconstruction with the surface atoms returning to its nearly perfect fcc nodes position. Similarly (001) facets are known to reconstruct quasi-hexagonally forming hexagonal patches on top of the square structure of the bulk[18]. Under chemisorption e.g. of CO the surface returns to its square form. At low coverages NO adsorbs on Pt atoms with NO bond perpendicular to the surface, at bridge positions wheras on-top positions are the most stable at high coverages. With increasing coverages surface sites are populated not sequentially moving to more weakly adsorbing sites[20,21]. Due to mutual NO interactions the adsorbate reorganizes at higher coverages with NO molecules tilting from vertical position minimizing their intermolecular repulsion[22]. Interacting NO molecules adsorbed at higher pressures and low temperatures form multilayer Pt coverage with dense chemisorbed adlayer fed by a more weakly bonded $(NO)_2$ species that slowly desorb but a multi-layer adsorption may remain up to 385 K[20]. A mechanism of the incorporation of NO to chemisorbed layer is unknown although the phenomenon was observed also for CO on Cu (100)[23]. Heating the adsorbate layer above 200K causes lifting the initial surface reconstruction what causes a two-fold increase in the number of top layer Pt atoms. The NO atoms from the depleted chemisorbed layer can thus move to a more energetically favourable bridge bonded sites. With further temperature rise the layer is ordering and finally NO desorbing[20].

The above experiments concern however in vacuo evolution. One can expect that at high NO pressure kept during the heating the scenario can differ as the adsorbate evolution depends even on the starting pressure during initial sorption[20]. With high pressure, high frequency collisions of NO with the surface the frequent adsorption-desorption phenomena may significantly modify the above picture. Using arguments from XRD analysis of a Pt surface we postulate here that the surface reconstruction occurs for Pt nanocrystals at temperatures 353-423 K under close to atmospheric pressure of NO. On missing-raw reconstruction the number of Pt atoms exposed to chemisorption per surface unit increases but the number of top layer Pt atoms decreases. This may weaken the adsorption leading to partial desorption of NO. An increasing strength of the remaining NO bonds may be however sufficient to lift the reconstruction. Such a feed back phenomena may lead to a semi-oscillatory behaviour driving high surface mobility and enabling quick coalescence of the collided nanocrystals even at relatively low temperatures. This possibility to our knowledge was never exploited in the literature and no experimental proof seems to exist.

The interaction of supported Pt clusters cannot be explained by magnetic forces although NO carries some magnetic moment. Bridge site adsorption of NO on (100) facets may effectively quench a magnetic moment of NO molecule whereas atop-site adsorption may leave residual NO magnetic moment on Pd(100) and may induce ferromagnetism on Pt and Pd that are paramagnetic in a bulk form[24]. The Curie temperature for this induced magnetism is however predicted to be rather low ($\leq 40K$)[25]. This and the occurrence of sintering at higher temperatures suggests its magnetic origin to be rather unlikely.

2 Experimental

In the presented study we have used samples of 10% (wt) Pt on amorphous silica (Davison 62, 100-120 mesh, 300 m^2/g).

The material was obtained by impregnation of silica with required amount of chloroplatinic acid following incipient wetness method. It was then mixed and dried. About 60 mg samples used for measurements were spread over a thin porous sintered glass disc and mounted vertically on a stainless steel heating block of our vacuum proof XRD camera. The environmental camera of 150 ml volume was similar to the described before[8], with removable cap having X-ray window secured by 12.5 μ m self adhesive Capton foil. It was connected to the gas line via Swagelok vacuum fittings and stainless steel flexible tubings enabling XRD measurements in Bragg-Brentano geometry. The outlet gas was collected from the back side of the porous glass through the heating block assuring close contact with the sample load. Between camera and the flex-tubing an union tee fitting (Swagelok) provided splitting the stream between output and a probing capillary of a mass spectrometer (Hiden Analytical). The gas feeding system consisted of pressured gas bottles and a gas line containing two stainless steel manifolds (A and B in Fig. 1) separated from the bottles entries and from a vacuum rotary pump by a normally closed on/off solenoid valves (1-12 in Fig. 1). The manifold outlets were fit with two mass-flow controllers (MKS1259C, 13-14 in Fig. 1) and their outlets linked into one steel line feeding the camera. The system enabled a clean switch of a supplied gas by pumping off the manifolds as well as a quick exchange of gases in the camera by its evacuating and flushing twice with the selected gas. The gases used were helium of 99.999% purity, hydrogen (99.9995%) and NO (99.5% purity with N_2, N_2O and CO_2 as a principal contaminants). The gas composition was recorded every 1-2 min. during repeating powder pattern collection in the angular range 20-140 deg. lasting 45 min per pattern. The mass spectrometer (MS) sample consisted of m/e scan from 1 to 50 using Faraday cup detector and second scan with SEM detector over m/e ranges having detected partial pressure lower than 10^{-7} atm. The time of one MS sample depended thus of a gas composition.

The temperature was controlled via two RE-15 controllers (Lumel) and the K-type thermocouples fitted to the heating camera block and to the front side of the porous glass disc.

The powder diffraction patterns were collected on D5000 powder diffractometer (Bruker AXS) equipped with LynxEye strip detector providing good resolution and quick data collection. The Cu K_α radiation has been employed with X-ray tube operating at 40kV and 40mA.

The whole setup was controlled by an integrated Linux client-server network architecture and the measurements could be repeatably performed under control of measurement scripts.

A control of gas purity after clean exchange of gases to He routinely shows a decaying low level of H_2 escaping from the stainless steel walls of the camera and low background of water. The oxygen contents remained at the level of several ppm. This level of contamination in the case of nanocrystals has much less effect than for single-crystal where 1 ppm of a contaminant may fully cover its surface. In nanocrystalline case the same level of impurities may affect only small percent of metal nanoparticles. The as prepared sample loaded into the camera has been dried in He at 50 deg.C for one day and then reduced in H_2 at the same temperature. The reduction progress was controlled via XRD showing slow transition of $PtCl_2$ phase (JCPDS card 85-0840) into Pt metal fcc phase. The appearance of $PtCl_2$ phase is in agreement with the suggested path of chloroplatinic acid hydrolysis to $PtCl_4(H_2O)_2$ proceeding slowly at RT during the material shelf life[26] . On drying, the dehydrated $PtCl_4$, having measurable vapor pressure, dissociates when heated, evolving chlorine[27] and depositing $PtCl_2$. In our procedure the reduction to metallic Pt was nearly complete after few hours but the sample was left in H_2 for one day. After the procedure few very weak maxima that could not be attributed to known crystallographic phase remain in the diffraction pattern. A conventional in catalysis procedure to stabilize sample by calcination at higher temperatures was applied to another sample and the results compared. At this stage as well as at the end of further 80 deg. treatment a part of the sample has been investigated by TEM (FEI Titan CUBED 80-300) in SEM mode as well as in high resolution.

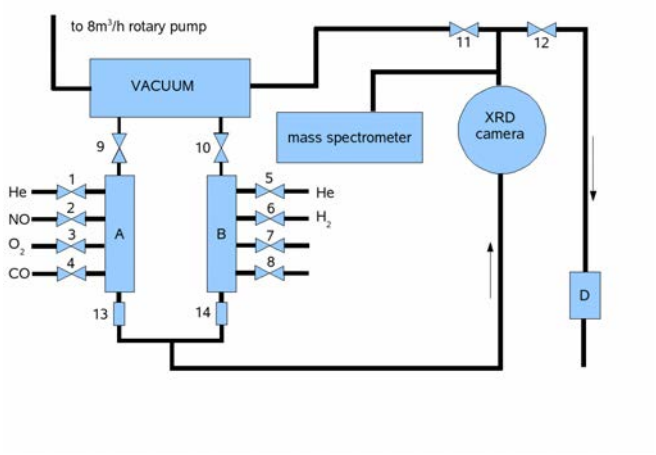

Fig. 1 XRD camera gas feeding system used in the experiments.

3 Results and Discussion

Williamson-Hall analysis[28] (W-H) of the XRD pattern of the reduced sample (Fig 2) results in Pt average crystallite size of 5.45 nm and a relatively small strain parameter of 0.002. For the size calculation we have used Scherrer constant equal to 1.03 resulting from direct comparison of several peaks width of a diffraction pattern calculated for model fcc metal cubooctahedra with the atomistic model size[6] . This size can be compared to the one from TEM analysis (Fig 3 e).

The images reveal quite uniform and narrow distribution of well separated Pt nanocrystals with average diameter of 3.56 nm. As XRD peak broadening analysis refers to the volume weighted average of the size distribution, the corresponding average is equal to :

$$D_V = \frac{\sum_{i=1}^{\infty} n_i d_i^4}{\sum_{i=1}^{\infty} n_i d_i^3}$$

where n_i is a fraction of crystallites of size d_i in the whole population of crystallites. For the presented distribution the D_V= 4.24 nm.

It may seem as a meaningful misfit, but to put this comparison

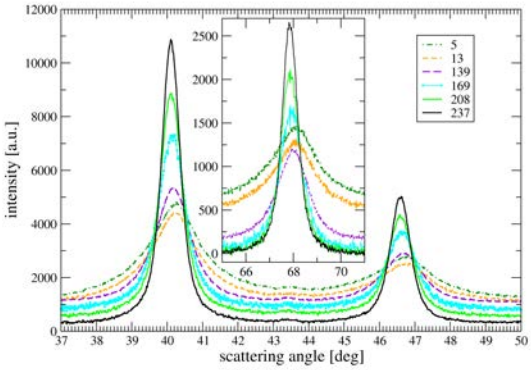

Fig. 2 Evolution of the 111, 200 and 220 diffraction peak during Pt/SiO_2 sample treatment. Legend refers to the pattern number of Fig.4.

on a realistic ground one has to notice that the volume average D_V quite strongly depends on very small changes of the distribution for higher sizes (e.g. $d_i > 10nm$). On the other hand the histogram data for this region is either missing or prone to substantial error as within the observed field there are only few (if any) larger crystallites and their statistics is poor. It can be a question of choice of the area to look at as well as a simple economy limiting number of TEM photographs to tens and not to hundreds. To illustrate this point Fig3 E together with the measured size histogram of 608 particles shows two lognormal distributions. Both fit well to the central part of the histogram and differ for larger sizes ($D > 5nm$) involving only 3% of counted particles. E.g. between 5 and 6 nm falls only 12 particles and the observed difference between the distributions equal to 40% corresponds to only 5 counted particles. If standard deviation (σ) of the counting statistics is proportional to square root of the count number then the observed difference between the distributions corresponds to less than 2σ what is common in counting phenomena. However the D_V values calculated for the presented lognormal distributions are 4.31 nm (2.78 nm the number average size - red curve) and 5.45 nm (2.88 nm the number average size -blue curve) respectively, the second one being in perfect fit with the XRD data.

The above discussion points to a different information that

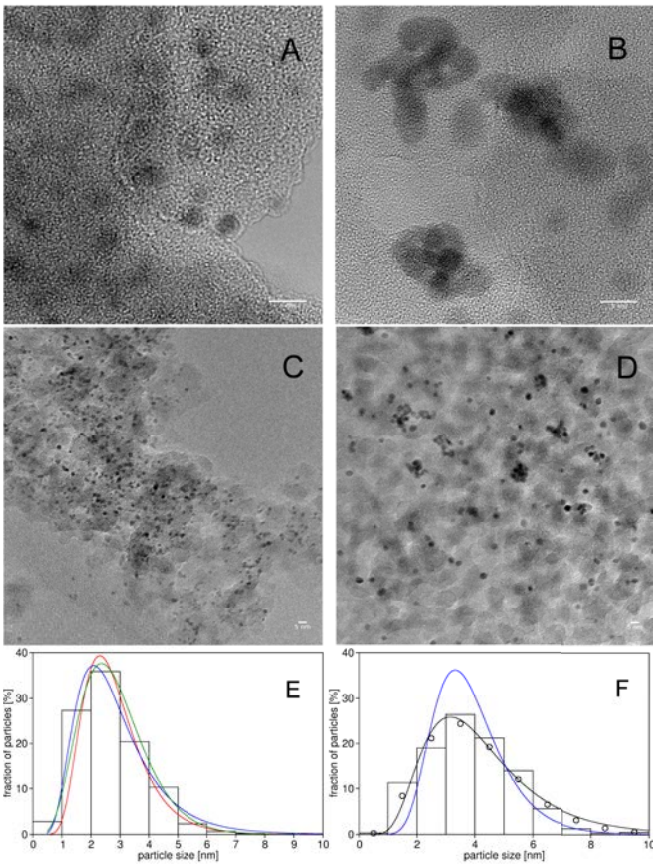

Fig. 3 TEM (A, B) and STEM (C, D) images with histogram of size (E, F) for the reduced sample (left) and the exposed to NO at 80 deg.C for two days (right). The particle size histograms include fit to a log-normal distribution (E, red curve, F - two fits: black and blue curve), to a log-normal distribution slightly modified to provide volume weighted average in agreement with XRD (E - blue curve) and to an exponential-power distribution (E - green curve, F - circles)).

can be obtained from XRD and TEM, where the former shifts its focus toward larger crystallite sizes if they exist in the studied sample. Different average particle sizes from both methods are thus quite common.

The reduced sample was subjected to the following treatment at 80 deg.C: (a) exposed to He stream (40 ml/min, 3h); (b) 16 cycles of: exposure to mixture of NO (20 ml/min) and He (20 ml/min) lasting 1 hour followed by flushing with He (40

ml/min) for 3 hours; (c) flushing with He (40 ml/min , 10 h); (d) exposure to NO (40 ml/min, 33 h). The temperature was then risen to 100 deg.C and (e) kept for the next 26 h in NO (20 ml/min) and He (20 ml/min) till no noticeable sintering was seen. Subsequently the sample was flushed with He (40 ml/min) and temperature was further increased to 120 deg.C then the sample was (f) kept in He for further 13.5 h and (g) exposed to NO (20 ml/min) and He (20 ml/min) for 25.5 h. It was followed by He flush (40 ml/min) and further temperature rise to 150 deg.C with the sample (h) kept for 22.5 h till no sintering noticed and (i) exposed to NO (20 ml/min) and He (20 ml/min) for 12.5 h till no further sintering observed.

The whole process lasting nearly 9 days was monitored by powder diffraction and MS with every pattern analyzed similarly as described before[8]. For each Pt fcc diffraction peak its position, intensity (peak amplitude and integral) and width (Full Width at Half Maximum - FWHM) was determined. All the analyzed parameters resulted from a procedure fitting the diffraction peaks to analytical profile[8]. As the data evolution for all reflections agree qualitatively, to minimize statistical scatter of the parameters, the peak positions for 111, 200 and 220 reflections were recalculated to a corresponding value of lattice constant and averaged. Fig.4 collects time evolution of these parameters, together with marked composition of the gas and temperatures. Fragments of the 111 peak width evolution (Fig.4 part C) at constant temperature have been fitted to the rate-power law curves that are further discussed.

Several phases of the above described gas and temperature treatment have been repeated on fresh samples of the catalyst to check repeatability. For the MS gas analysis the same treatment has been applied to the clean porous glass disc mounted in the camera for a blind test.

During NO cycles at the beginning of the experiment at 80 deg.C only small amount of NO dissociates with evolution of N_2O (m/e=44, Fig.5). After 3rd cycle O_2 (m/e=32) appears in growing quantities quickly arriving at the level of approximately half of the N_2O emission in agreement with a global stoichiometry N:O = 1:1. The lacking amount of oxygen agrees roughly with the sorption capacity of silica. From the m/e=32 MS signal level the 0.002 of the level of NO signal has been subtracted as NO fragmentation involves m/e=32 with that small intensity. The minimum level of m/e=44 (dashed line) agrees well with the blind test m/e=44 content in the pressured bottle. A growth of a small quantities of NO_2 (m/e=46) to the level of 0.05% of that of NO is also noticeable from Fig.5. Fig.5 covers the gas composition evolution from the beginning up to the pattern number 130 in Fig.4. Note the nonlinearity of the MS sampling rate with time, the latter being dependent on the gas composition.

Analyzing Fig.4 (A) one can notice a slight shift of the lattice parameter (LP) by 0.003 Å(on average) upward on cyclic exposition to NO at 80 deg.C (phase b). Switching the gas composition from NO to He should not cause quick desorption of a strongly bonded NO at this temperature. E.g. TPD experiments suggest NO desorption occurring above 150 deg.C[29]. This is why we do not interpret the shift up as manifestation of the adsorption phenomenon. The visible mark of the adsorption is an upward shift of the measured LP, in agreement with a simple model where adsorption saturates the surface bonds and causes expansion of the contracted surface layer increasing the average LP - the model positively tested in our laboratory on many examples. The downward shift is however visible at the beginning of phase (h) at 150 deg.C, which is interpreted as slow (3 h) desorption of NO ended up by reconstruction of the surface with the LP shifted up. It is accompanied by rise of the peak height in agreement with analogous observation of the process of Pt surface reconstruction on desorption of hydrogen[8]. Here the NO desorption is slow

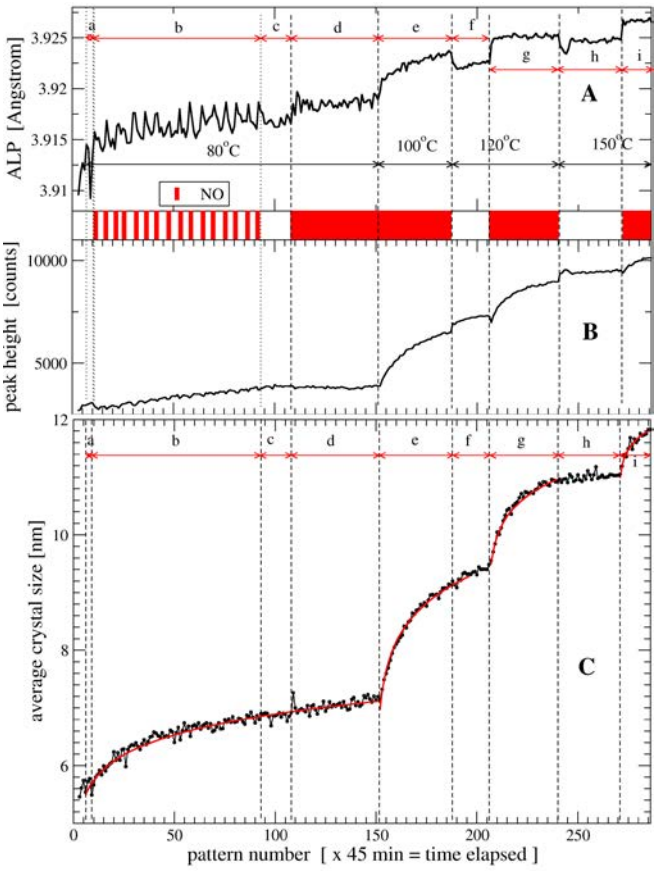

Fig. 4 Evolution of Pt fcc phase control parameters of powder diffraction pattern . ALP is an apparent lattice parameter as obtained from the peak position (A), peak height is Pt 111 peak amplitude (B) and average crystal size is the measured FWHM of Pt 111 recalculated to size via Scherrer formula. Red lines are the results of the rate-power law fit.

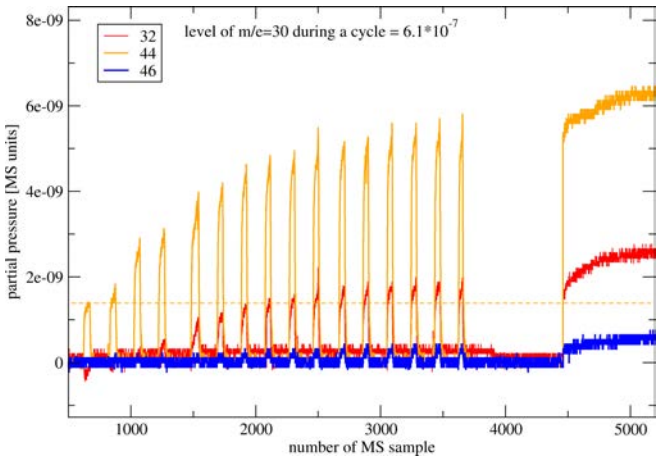

Fig. 5 MS sampling of the gases outgoing from of the camera. Only residual gases shown with partial pressure of NO being about $6.1 * 10^{-7}$ atm.

as running slightly below the thermodynamic temperature of desorption. Then, it is natural to interpret the cyclic LP shift up as a reconstruction of the Pt crystallites surface.

The observed phenomenon evidently concerns only surface of the monitored Pt fcc phase. The shift up of LP signifies then expansion of the Pt nanocrystal surface. It does not affect scattered intensity (Fig.4 B) changing only due to gas x-ray absorption, so the observed structural transformation is not due to a deepening disorder of the surface. The measured effect is of just the same magnitude as observed by us before for surface reconstruction during H_2 desorption.

It is known, as stated in the introduction, that a multilayer adsorption of NO at high pressures causes shift of NO molecules from strongly to more weakly bonding sites while increasing a number of bonded molecules[20]. It may weaken the interaction with the surface to the point when it starts to behave like a clean surface and reconstruct or may interact specifically promoting reconstruction. Exposition to He would cause weakly bonded NO to desorb with the remaining molecules moving back to the strongly bonding sites - the process lifting the reconstruction and moving the surface Pt atoms back to their lattice nodes.

In our study of Pt nanocrystals reconstruction during desorption of H_2[8] its effect on a diffraction peak position has been measured. For about 4.5 nm Pt crystallites and temperature of 100 deg.C we recorded shift of the 111 reflection on reconstruction by about 0.1 deg. corresponding to 0.01Å shift in LP. The analogous shift of LP for Pt 3.1 nm crystallites was 0.02Å (Fig.7 of[8]). As square of sizes ratio is 1:2, its decrease with the nanocrystal size is expected to be inversely proportional to the average nanocrystal surface. From Fig.4 A we can estimate LP shift for the beginning of phase (b) (estimated size 5.65 nm), transition from the phase (c) to (d) (size 6.95 nm), at 120 deg.C (size 9.45 nm), and at 150 deg.C (size 11.05 nm). These values: 0.003(4)Å, 0.0018(8)Å, 0.0024(3)Å, 0.0018(4)Å correspond to expected from the growing surface: 0.0064Å, 0.0042Å, 0.0023Å, 0.0017Å respectively. The figures in parentheses give standard deviation of the last figure estimated from averaging LP values over 10 points before and after the shift edge. The observed LP shift is about half of the expected for small nanocrystals and agree with the expected for larger sizes. As the expected values correspond to a full surface reconstruction it suggests that we do not observe full reconstruction of the whole Pt surface, various fragments dynamically changing their state. The observation that the LP shift approaches its expected value for larger crystallites may be due to its growing surface with decreasing fraction being in contact with other coalescing particles. Thus an increasing with size fraction of the surface undergoes reconstruction.

The LP (Fig.4 part A) at phase (e) shows marked increase during quick crystallite growth. This effect has been discussed before[6]. The further evolution of the LP agrees well with the temperature lattice expansion of Pt assumed to be $8.8 \cdot 10^{-6} K^{-1}$.

Section B of Fig.4 shows evolution of the 111 peak amplitude. The rate of growth is highly correlated with the estimated crystallite size i.e. inversely proportional to FWHM. The curve was not corrected for the X-ray absorption by gas in the camera but the visible oscillations as well as shifts on gas exchange are well described by this varying absorption of gas and are not interpreted structurally.

Section C of Fig. 4 presents evolution of the average crystallite size estimated directly from the FWHM using Scherrer formula. The routine did not account for the material strain. To check its effect for several patterns the full range W-H analysis has been done, showing approximately constant strain parameter. This analysis provides also slight correction to the presented in section C values. No instrumental broadening was considered as for the studied particle sizes it provides negligible correction.

As the W-H correction is nearly constant, the values from Fig.4 C were used to fit the phases of quick growth (b-c-d, e, g, i) to the rate-power law of the form:

$$\frac{dS}{dt} = -K_S S^n$$

where S is the exposed metal surface and K_S is constant. This can be rewritten in the form:

$$\frac{dD}{dt} = K_D D^{2-n}$$

where D is the mean particle diameter $D = 6V/S$, $K_D = K_S(6V)^{n-1}$. This can be easily solved to the form: $D(t) = ((n-1)K_D t + C)^{\frac{1}{n-1}}$. The mean D in the formula above is

a surface weighted average that differs from both: number weighted value (directly from TEM) and volume weighted average, as comes from Scherrer formula and XRD data. Assuming log-normal distribution of crystallite size that widens during the process, we have tested several approximations to follow evolution of the surface weighted size average. However the best fit powers do not depend strongly on these approximation as their evolution remains very similar, and the same set of values could be kept.

The best fit to the rate-power law results in the following powers: phase (b-c-d) , n=14; phase (e), n=13; phase (g), n=20 and phase (i), n=40. These values for the initial process are similar to observed for coalescence at 700 deg.C[30] but for the following growth are significantly higher than the reported in literature (typically 4-5)[30] suggesting that the particle growth is very quick and its mechanism differs from normally observed diffusion driven growth. They also suggest that the mechanism of growth changes after phase (e), when possibly diffusion mechanism starts to dominate. The value of rate power does not necessary characterize a simple process. In practice quite complex sequence of processes affecting sintering may change its value[26].

At the end of phase (d) a part of the sample has been analyzed by TEM and Fig.3 shows its representative pictures (B, D, F) compared with the initial sample after reduction (phase (a) - A, C, E). The tendency for Pt nanocrystals to group in clusters is striking. Linking this with the observed by XRD mean crystallite growth brings natural conclusion that the coalescence is the growth rate determining phenomenon up to the phase (d). Considering evolving powers of the rate-power law, it probably dominates also during phase (e).

A quick growth of Pt nanocrystals supported on silica has been observed in our laboratory many times in various experimental setups. Fig.6 shows an example of a quick sintering in NO atmosphere at temperature 200 deg.C measured using position sensitive detector INEL CPS120. The fresh sample was calcined in O_2 at 400 deg.C and reduced in H_2 at 500 deg.C during 6 h with Pt crystallites size about 8 nm. Then the sample was briefly flushed with helium at 200 deg. C and exposed to NO (20 ml/min). The presented diagrams are rather noisy but the effect of surface reconstruction is clearly visible accompanied with quick crystal growth with fitted rate power n=6. It suggests that the actual mechanism of growth can be modified but the process is always observed together with reconstruction phenomena. Interestingly Fig.6 suggests also slight shape anisotropy of the Pt nanocrystals with maximum size in 111 direction. This was also the direction of the quickest growth.

The experimental data presented above not fully explain the precise atomistic mechanism of the observed coalescence. An answer to the question why it occurs for Pt but was never observed for Pd may lay in a specific to Pt mechanism of nanocrystal transport as well as in specific to Pt mechanism

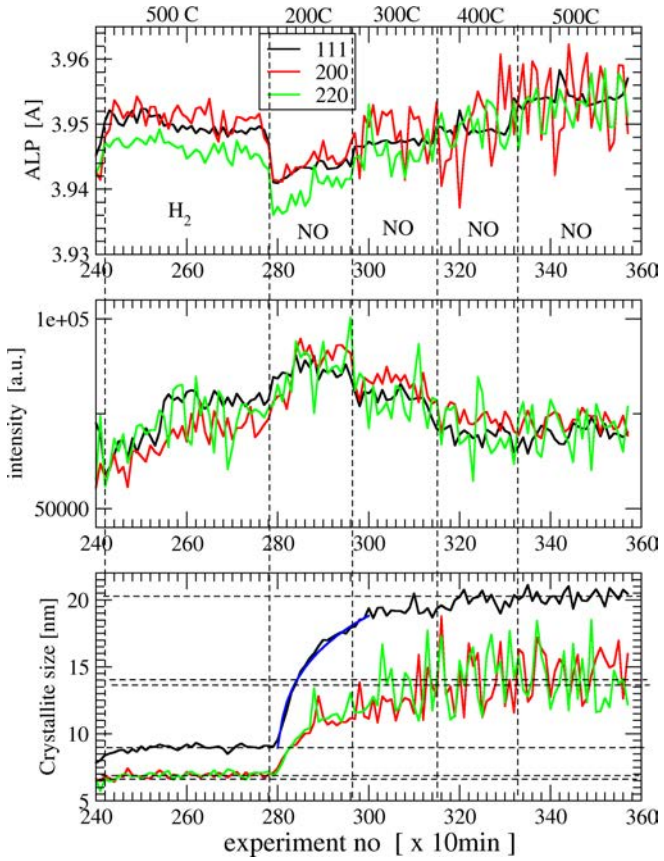

Fig. 6 An example of quick sintering for calcined 10% Pd/SiO_2 kept in NO at 200 deg.C.

of growth of the collided nanocrystals. On collision the collided surfaces should easily link as the chemisorption energies of NO reported in literature[31,32] are by far lower than the Pt cohesion energy. The cohesive energy of Pd is lower (3.94 eV versus 5.86 eV for Pt) but still larger than chemisorption energies of NO (in the range 1-2 eV). A further buildup of a larger nanocrystals requires however substantial mass transport and this may be provided by the reconstructing surfaces. The number of atoms exposed on reconstructed and unreconstructed surfaces is different and the phenomenon should involve mass transfer. It can be speculated that the reconstruction may cause desorption of a part of the sorbed NO, that can move to a stronger bonding sites. It could then trigger lifting of the reconstruction initiating cyclic surface rearrangement. This should provide efficient mechanism for motion of the whole clusters over the support. A traditionally considered one is a nucleation of new monoatomic layers of the crystal facets, with its rate estimated from nucleation theory[9]. But the surface reconstruction provides the necessary movement of surface atoms. The traditionally considered coalescence could provide sufficient mobility to 6 nm Pt nanocrystals on

support at temperatures above 600 deg.C[26,30]. This is why it was rejected in literature as a possible factor affecting Pt sintering at low temperatures[9]. However the reconstruction phenomena can provide both: mechanism of cluster transport and a mechanism of growth.

Some light on the atomistic mechanism of sintering can be shed by TEM observations of Pd nanocrystal after heating in NO. If the mechanism is limited only to 5d transition metals, also the experiments on Ir supported on silica can add to an understanding of the phenomenon. Such experiments are in preparation. The observed by XRD shifts of the measured peak position agree very well with the studied by us reconstruction of the Pt nanocrystal surface and we know no other phenomenon that could explain such behavior. Shift in the diffraction peak position is always connected with changing distribution of atoms in the observed crystallographic phase. We observed cyclic shifts on exposition to NO conserving the fcc ordering. It is natural to ascribe them to surface phenomena.

Crucial for the interpretation is the assumption that NO does not quickly desorb at 80 deg.C. TPD studies e.g.[29] with the heating rate 7K/s, report desorption of NO at above 150 deg.C. and possibly higher for very small nanoparticles. The desorption peak has however significant width and the desorption with low rate can be observed even below the desorption temperature. In our case the process was already sufficiently slow at 150 deg.C to be observed over several hours with characteristic marks of surface reconstruction at the final stage.

The observed low temperature growth is specific to Pt. It was never observed below 80 deg.C and it is postulated here that the reconstruction provides crucial mechanism driving quick coalescence at low temperatures.

4 Conclusions

The presented results from TEM as well as from an operando XRD/MS study provide strong evidence that the low temperature, quick growth of Pt nanoparticles supported on silica, exposed to NO, results from coalescence. As coalescence in catalysis is known as a high temperature phenomenon, this opens up a question about a possible mechanism of the low temperature coalescence. Our former experience in observation by XRD of reconstruction of Pt nanoparticles surface on desorption of H_2[8] allows us to understand the peak position evolution in NO. It implies reconstruction of Pt surface occurring at high pressure coverage of NO. Such reconstruction at high pressure of NO at temperatures above 80 deg.C is yet unknown phenomenon. Known phenomena of surface reconstruction of Pt involve significant movement of atoms. If the reconstructed surface changing number and energetics of chemisorption sites, desorbs part of a weakly bonded NO, that may lift the reconstruction providing necessary feed back for the surface mobility. This may pose sufficient drive to move whole Pt clusters over the support as well as means to build up a larger crystallite out of two smaller collided. The proposed mechanism needs further confirmation both experimentally and theoretically. This low temperature coalescence could be used for a controlled Pt growth with a predictable size distribution or in selective growth of Pt nanocrystals in mixtures. The phenomenon and its mechanism is new and was never reported in the literature.

5 Acknowledgment

The work has been financially supported by The Polish National Science Center (NCN) under Research Grant No N N204 097839.

References

1 Somorjai, A.G.; Park, J.Y. Physics Today **2007** Oct., 48-53.
2 Freund,H.J.; Kuhlenbeck,H.; Libuda,J., Rupprechter,G.; Baumer,M.; Hamann H. Topics in Catalysis **2001**, 15, 201-209.
3 Su,X.C.; Cremer,P.S.; Shen,Y.R.; Somorjai,G.A. J.Am.Chem.Soc. **1997**, 119, 3994-4000.
4 Thostrup,P., Vestergaard,E.K., An,T., Lgsgaard,E., Besenbacher,F. J. Chem. Phys. **2003**, 118, 37243730.
5 Vang,R.T., Lgsgaard,E., Besenbacher,F. Phys.Chem.Chem.Phys. **2007**, 9, 34603469.
6 Kaszkur, Z. J.Appl.Cryst. **2000**, 33, 87-94.
7 Kaszkur, Z. J.Appl.Cryst. **2000**, 33, 1262-1270.
8 Rzeszotarski, P.; Kaszkur, Z. Phys.Chem.Chem.Phys. **2009**, 11, 5416-5421.
9 Lööf, P.; Stenbom, B.; Norden, H.; Kasemo, B. J.Catal. **1993**, 144, 60-76.
10 Handforth, S.L.; Tilley, J.N. Ind.Eng.Chem. **1934**, 26, 1287-1292.
11 Taylor, H.S. J.Phys.Chem. **1926**, 30, 145-171.
12 Ruckenstein, E.; Pulvermacher, B. J.Catal. **1973**, 29, 224-245.
13 Banholzer, W.F.; Park, Y.O.; Mak, K.M.; Masel, R.I. Surf.Sci. **1983**, 128, 176-190.
14 Hong, Wang; Tobin, R.G.; DiMaggio, C.L.; Fisher, G.B.; Lambert, D.K.; J.Chem.Phys. **1997**, 107, 9569-9576.
15 Parkyns,N.D. Proc.5th Int.Congress on Catalysis **1972**,(12), 255-264.
16 Loffreda, D.; Simon, D.; Sautet, P. J.Chem.Phys. **1998**, 108, 6447-6457.
17 Ho, K.-M.; Bohnen, K.P. Phys.Rev.Lett. **1987**, 59, 1833-1836.
18 Titmuss, S.; Wander, A.; King, D.A. Chem.Rev. **1996**, 96, 1291-1305.
19 Chan, C.-M.; van Hove, M.A.; Weinberg, W.H.; Williams E.D. Solid State Commun. **1979**, 30, 47-49.
20 Brown, W.A.; Sharma, R.K.; Ge, Q.; King, D.A. Phys.Chem.Chem.Phys. **1999**, 1, 1995-2000.
21 Backus, E.H.; Eichler, A.; Grecea, M.L.; Kleyn, A.W.; Bonn, M. J.Chem.Phys. **2004**, 121, 7946-7954.
22 Hammer, B.; Norskov, J.K. Phys.Rev.Lett. **1997**, 79, 4441-4444.
23 Cook,J.C.; McCash;E.M. Surf. Sci. **1996**, 356, L445.
24 Hass, K.C.; Tsai, M.-H.; Kasowski, R.V. Phys.Rev.B **1996**, 53, 44-47.
25 Mulhollan, G.A.; Fink, R.L.; Erskine, J.L. Phys.Rev.B **1991**, 44, 2393-2395.
26 Anderson, J.R. Structure of Metallic Catalysts, Academic Press 1975, p182.
27 Dorling, T.A.; Lynch, B.W.J.; Moss, R.L. J.Catal. **1971**, 20, 190-201.

28 Williamson, G.K.; Hall, W.H. Acta Metall. **1953**, 1, 22-31; Mote, V.D.; Purushotham, Y.; Dole, B.N. J.Theor.Appl.Phys. **2012**, 6:6.
29 Altman, E.I.; Gorte, R.J. J.Phys.Chem. **1989**, 93, 1993-1997.
30 Harris,P.J.F. Int.Mater.Rev. **1995**, 40, 97-115.
31 Brown, W.A.; King, D.A. J.Phys.Chem.B **2000**, 104, 2578-2596.
32 Tang, H.; Trout, B.L. J.Phys.Chem.B **2005**, 109, 17630-17634.